Published in final edited form as:

*Arterioscler Thromb Vasc Biol*. 2018 April ; 38(4): e36–e47. doi:10.1161/ATVBAHA.117.310656.

# RGC-32 deficiency protects endothelial cell from inflammation and attenuates atherosclerosis

**Xiao-Bing Cui**[1], **Jun-Na Luan**[1], **Kun Dong**[1], **Sisi Chen**[1,2], **Yongyi Wang**[3], **Wendy T. Watford**[4], and **Shi-You Chen**[1,2,*]

[1]Department of Physiology & Pharmacology, University of Georgia, Athens, GA

[2]Department of Endocrinology, Renmin Hospital, Hubei University of Medicine, Shiyan, Hubei, China

[3]Department of Cardiovascular Surgery, Renji Hospital, School of Medicine, Shanghai Jiaotong University, Shanghai, China

[4]Department of Infectious Diseases, University of Georgia, Athens, GA

## Abstract

**Objective—**The objective of this study is to determine the role and underlying mechanisms of response gene to complement 32 (RGC-32) in atherogenesis.

**Approach and Results—**RGC-32 was mainly expressed in endothelial cells (ECs) of atherosclerotic lesions in both apolipoprotein E-deficient ($ApoE^{-/-}$) mice and human patients. RGC-32 deficiency ($Rgc32^{-/-}$) attenuated the high-fat diet-induced and spontaneously developed atherosclerotic lesions in $ApoE^{-/-}$ mice without affecting serum cholesterol concentration. $Rgc32^{-/-}$ appeared to decrease the macrophage content without altering collagen and smooth muscle contents or lesional macrophage proliferation in the lesions. Transplantation of wild-type (WT) mouse bone marrow to lethally irradiated $Rgc32^{-/-}$ mice did not alter $Rgc32^{-/-}$-caused reduction of lesion formation and macrophage accumulation, suggesting that RGC-32 in resident vascular cells, but not the macrophages, plays a critical role in the atherogenesis. Of importance, $Rgc32^{-/-}$ decreased the expression of intercellular adhesion molecule 1 (ICAM-1) and vascular cell adhesion molecule 1 (VCAM-1) in ECs both *in vivo* and *in vitro*, resulting in a decrease in tumor necrosis factor (TNF)-α-induced monocyte-EC interaction. Mechanistically, RGC-32 mediated the ICAM-1 and VCAM-1 expression, at least partially, through nuclear factor (NF)-κB signaling pathway. RGC-32 directly interacted with NF-κB and facilitated its nuclear translocation, and enhanced TNF-α-induced NF-κB binding to ICAM-1 and VCAM-1 promoters.

**Conclusions—**RGC-32 mediates atherogenesis by facilitating monocyte-EC interaction via the induction of endothelial ICAM-1 and VCAM-1 expression, at least partially, through NF-κB signaling pathway.

*Corresponding author: Shi-You Chen, PhD, Department of Physiology & Pharmacology, The University of Georgia, 501 D.W. Brooks Drive, Athens, GA 30602, Tel: 706-542-8284, Fax: 706-542-3015, sc229@uga.edu.

**Disclosures:** None.

**Keywords**

response gene to complement 32; atherosclerosis; endothelial cells; adhesion molecules; nuclear factor-κB

**Subject code**

Atherosclerosis; Cardiovascular Disease; Inflammation

## Instruction

Atherosclerosis is a major cause of coronary artery disease, stroke, and peripheral vascular diseases. Atherosclerotic lesion is characterized by the accumulation of lipid particles and immune cells in the subendothelial space, resulting in narrowing of the arterial lumen. Endothelial cell (EC) activation upon exposure to oxidized lipids and proinflammatory stimuli, such as tumor necrosis factor (TNF)-α, plays an important role in the initiation and progression of atherosclerosis.[1, 2] Activated ECs express adhesion molecules, such as intercellular adhesion molecule 1 (ICAM-1) and vascular cell adhesion molecule 1 (VCAM-1), and mediate the interaction between leukocytes and vascular ECs, which is critical for the atherogenesis.[3–6]

Nuclear factor (NF)-κB is an important regulator of endothelial ICAM-1 and VCAM-1 expression.[7–10] Both ICAM-1 and VCAM-1 promoters contain NF-κB binding sites.[11, 12] Remarkably, EC-specific NF-κB inhibition abrogates adhesion molecule induction in ECs, impairs macrophage recruitment to atherosclerotic plaques, and protects mice from atherosclerosis,[13] indicating the critical role of endothelial NF-κB signaling in the pathogenesis of atherosclerosis. However, the factors that regulate NF-κB function in ICAM-1 and VCAM-1 transcription remain largely unknown.

Response gene to complement 32 (RGC-32) is expressed in numerous organs and tissues and functionally involved in cell proliferation,[14, 15] differentiation,[16] and cancer.[17–19] It is induced by p53 in glioma and forms a protein complex with polo-like kinase 1 leading to G2/M arrest.[20] It also mediates transforming growth factor-β-induced epithelial-mesenchymal transition in human renal proximal tubular cells through interacting with Smad3.[21, 22] Recent studies from our laboratory show that RGC-32 expression is induced in mouse adipose and liver tissues with high-fat diet (HFD) challenge. RGC-32 deficiency ($Rgc32^{-/-}$) protects mice from HFD-induced obesity and hepatic steatosis,[23, 24] suggesting that RGC-32 plays an important role in inflammatory and metabolic disease. A recent study indicates that RGC-32 is expressed in the human atherosclerotic arterial wall and mediates C5b-9-induced vascular EC proliferation and migration.[25] Whether or not RGC-32 plays a functional role in atherosclerosis and endothelial inflammation, however, remains to be determined.

In the present study, we found that RGC-32 is induced predominantly in ECs of atherosclerotic lesions and promotes the development of atherosclerosis. RGC-32 appears to

mediate monocyte-EC interaction by stimulating the expression of endothelial ICAM-1 and VCAM-1, at least partially, via NF-κB signaling pathway.

## Materials and Methods

### Animals

The wild-type (WT) C57BL/6 mice were purchased from the Jackson Laboratory (Bar Harbor, ME, USA). $Rgc32^{-/-}$ mice on the C57BL/6 background were generated and genotyped as described previously.[26] $Rgc32^{-/-}$ mice were bred with C57BL/6 apolipoprotein E-deficient ($ApoE^{-/-}$) mice (Jackson laboratories) to generate $ApoE^{-/-}Rgc32^{-/-}$ mice. Eight-week-old male $ApoE^{-/-}$ or $ApoE^{-/-}Rgc32^{-/-}$ mice were fed a HFD (D12108C, Research Diets Inc) for 12 weeks or normal chow diet for 1 year for atherosclerotic lesion development. All animals we used in this study were male and housed under conventional conditions in the animal care facilities, and received humane care in compliance with the Principles of Laboratory Animal Care formulated by the National Society for Medical Research and the Guide for the Care and Use of Laboratory Animals. All experimental procedures were approved by the Institutional Animal Care and Use Committee (IACUC) of The University of Georgia.

### Human atherosclerosis specimen collection

Human atherosclerotic plaque specimens were obtained from the patients undergoing off-pump coronary artery bypass grafting (CABG) surgery at the Department of Cardiovascular Surgery, Renji Hospital, School of Medicine, Shanghai Jiaotong University. The study was approved by Renji Hospital Ethics Committee and performed in accordance with the ethical standards.

### Atherosclerotic lesion analysis and metabolic profiling

Mice were anesthetized using 2% isoflurane inhalation. Body weight was recorded, and blood was withdrawn by cardiac puncture. Serum was prepared and analyzed for triglyceride, cholesterol, and PCSK9 concentration using Triglyceride Quantification Kit (Abcam, ab65336), HDL and LDL/VLDL Cholesterol Assay Kit (Abcam, ab65390), and Human PCSK9 Picokine™ ELISA Kit (Boster Biological Technology, EK1147), respectively following the manufacturer's instructions as described previously.[23] Mouse hearts with aortic roots, whole aortas and livers were harvested. For *en face* plaque analyses, the aortas were opened longitudinally, fixed in 4% paraformaldehyde overnight, stained with oil red O for 1 hour, and rinsed with 70% ethanol. The hearts with the aortic roots were embedded in OCT compound, and 10 μm mouse aortic root sections were stained with Oil Red O as described.[27] Images were viewed and captured by a Nikon microscope. The atherosclerotic lesion areas were quantified using ImageJ. Oil Red O staining of the frozen liver sections (10 μm) and quantitative analysis were performed as described previously.[24, 27] Liver triglyceride content was determined using Triglyceride Quantification Kit (Abcam, ab65336) following the manufacturer's instructions.

## Cell Culture

Mouse aortic ECs and smooth muscle cells (SMCs) were isolated and cultured as previously described.[28, 29] Briefly, mice were anesthetized using 2% isoflurane inhalation. The midline of the abdomen was incised, and the thorax opened to expose the heart and lungs. The abdominal aorta was cut at the middle to release the blood, and then perfused with 1 ml of PBS containing 1,000 U/ml of heparin from the left ventricle. The aorta was dissected out from the aortic arch to the abdominal aorta, and immersed in DMEM containing 20% FBS and 1,000 U/ml of heparin. The fat or connecting tissue was rapidly removed with fine forceps under a stereoscopic microscope. A 24-gauge cannula was inserted into the proximal portion of the aorta. After ligation at the site with a silk thread, the inside of the lumen was briefly washed with serum-free DMEM. The other side was bound and filled with collagenase type II solution (1 mg/ml, dissolved in serum-free DMEM, Worthington Biochemical Corporation, LS004176). After incubation at 37 °C for 45 minutes, adventitia was removed from the artery using two fine forceps under a dissecting microscope. ECs were removed from the aorta by flushing with 5 ml of DMEM containing 20% FBS. ECs were collected by centrifugation at 1,200 rpm for 5 minutes, and the precipitate was gently resuspended by pipette with 2 ml of DMEM with 20% FBS and cultured in a 35 mm type I collagen-coated dish. After incubation at 37 °C for 2 hours, the medium was removed, and the cells were washed with warm PBS. Then, medium G (20% FBS (Atlanta Biologicals, S11550H), 100 U/ml penicillin-G, 100 μg/ml streptomycin (Hyclone, SV30010), 2 mM L-Glutamine (Corning, 25-005-CI), 1 × non-essential amino acids (Sigma, M7145), 1 × sodium pyruvate (Sigma, S8636), 25 mM HEPES (pH 7.0–7.6) (Sigma, H0887), 100 μg/ml heparin, 100 μg/ml ECGS (Sigma, E2759), and DMEM) was added. For SMC isolation, the artery was incubated in DMEM with 10% FBS overnight, followed by incubation with 1 mg/ml collagenase type II and 0.5 mg/ml elastase (Sigma, E-0258) at 37 °C for 30 min. The artery was gently triturated with a 1 ml pipette, and then 10 ml of the culture medium was added to terminate the digestion. Cells were collected by centrifugation at 1,800 rpm for 10 minutes, and the precipitate was gently resuspended in DMEM containing 10% FBS and cultured under 37 °C in a 5% $CO_2$ condition.

Human umbilical vein endothelial cells (HUVECs) were purchased from Lifeline Cell Technology (FC-0003) and cultured using VEGF endothelial medium (LL-0003) under 37°C, 5% $CO_2$ conditions. The cells at passages 3 to 5 were used in this study.

The cultured cells were treated with vehicle or 20 ng/ml of TNF-α (Sigma, GF023) for indicated times without starvation.

## Quantitative Real-Time PCR

Total RNA was isolated from cultured ECs or SMCs with TRIzol reagent (Invitrogen, Carlsbad, CA, USA, 15596018). 1 μg of total RNA was reverse-transcribed using the iScript cDNA Synthesis kit (Bio-Rad, #1708891). The cDNA was then subjected to quantitative PCR (qPCR) with All-in-One qPCR Mix (GeneCopoeia, QP001) using the Mx3005P qPCR machine as described previously.[26] Each sample was amplified in triplicate. The expression of each gene was normalized with cyclophilin. The primers used are listed in Online Table I.

### Western blot analysis

Primary cultured ECs, SMCs, or HUVECs were washed twice with PBS followed by protein extraction using RIPA buffer (50 mmol/L Tris-HCL, pH 7.4, 1% Triton X-100, 0.25% wt/vol sodium deoxycholate, 150 mmol/L NaCl, 1 mmol/L EGTA, 0.1% SDS) containing protease inhibitors (Thermo Scientific, 78428). The protein concentration was measured using BCA Protein Assay Reagent (Thermo Scientific, 23225). Lysates were denatured by boiling in gel loading buffer containing SDS and 2-mercaptoethanol solution. Cell lysates were resolved on a 9% or 12% SDS-PAGE and then transferred to polyvinylidene difluoride (PVDF) membranes (Bio-Rad, 1620177). Membranes were blocked with 5% skim milk and then incubated with primary antibodies at 4 °C overnight followed by incubation with HRP-conjugated secondary antibody (Sigma) at room temperature for 1 hour. Protein expression was detected with an enhanced chemiluminescence (Millipore, WBKLS0500). Antibodies against RGC-32 (1:1000), ICAM-1 (1:1000, Abcam, ab124760), VCAM-1 (1:1000, Abcam, ab134047), P-selectin (1:1000, Abcam, ab178424), phospho-NF-κB p65 (1:1000, Cell Signaling Tech, 13346S), NF-κB p65 (1:1000, Cell Signaling Tech, 8242S) and α-tubulin (1:1000, Sigma, T6074) were used for immunoblotting.

### Histochemistry and immunohistology analysis

After fixing in 4% paraformaldehyde overnight, the hearts with aortic roots were dehydrated in a graded series of ethanol and xylene solutions, embedded in paraffin, and sectioned (5 μm). The sections were deparaffinized in xylene and rehydrated. Collagen content in the lesion was measured using a Masson's Trichrome Staining Kit (American MasterTech, KTMTR2) by following the manufacturer's instruction. In order to measure fibrous cap thickness, at least 3 measurements of the thinnest fibrous cap within one atherosclerotic plaque were taken and averaged as described previously.[30] For immunohistochemistry staining, the sections underwent microwave antigen retrieval in 10 mM citrate buffer (pH 6.0), allowed to cool down to room temperature, and washed with PBS. The endogenous peroxidase activity was quenched by the addition of 3% $H_2O_2$. Subsequently, slides were washed with PBS, and non-specific antibody binding was blocked by incubation with 10% goat serum for 30 min at room temperature. The sections were then incubated with RGC-32 (1:200), α-smooth muscle actin (α-SMA) (1:200, Sigma, A5228), CD68 (1:200, Bio-Rad, MCA1957), ICAM-1 (1:200, Abcam, ab124760), VCAM-1 (1:200, Abcam, ab134047) primary antibody, or corresponding normal IgG (negative control) at 4 °C overnight followed by incubation with horseradish peroxidase-conjugated secondary antibody. The sections were counterstained with Hematoxylin. Images were captured with a CCD camera mounted on a Nikon microscope. Quantification was performed using ImageJ Immunohistochemistry Image Analysis Toolbox. For immunofluorescent staining, the hydrated sections underwent microwave antigen retrieval as described above, washed with PBS, and blocked with 10% goat serum for 30 min at room temperature, followed by incubation with RGC-32 (1:100), CD31 (1:100, Santa Cruz Biotechnology, sc-365804), α-SMA (1:100, Sigma), CD68 (1:100, Bio-Rad, MCA1957), Ki67 (1:100, Abcam, ab16667) primary antibody, or corresponding normal IgG (negative control) at 4 °C overnight. Then, the sections were incubated with FITC- (1:100) or TRITC-labelled (1:50) secondary antibody at room temperature for 1 hour. Nuclei were stained with 4, 6-diamidino-2-

phenylindole (DAPI, Vector Laboratories, H-1500). Fluorescent images were captured using a Nikon fluorescent microscope.

Cell immunofluorescence was performed as described previously.[26] HUVECs were cultured on glass coverslips and treated as indicated. Then the cells were fixed with 4% paraformaldehyde, permeabilized with 0.2% Triton X-100 in PBS and incubated with 10% normal goat serum for 30 minutes at room temperature. The cells were incubated overnight at 4 °C with anti-NF-κB p65 (1:100) or anti-RGC-32 (1:100) primary antibody, and then TRITC-labelled (1:50) secondary antibody for 1 hour at room temperature. Nuclei were stained with DAPI. Fluorescence images were captured by a Nikon fluorescent microscope. Quantification analysis was performed using ImageJ.

## Bone barrow transplantation

Eight-week-old male WT and Rgc32$^{-/-}$ recipient mice were lethally irradiated with 1100 rad 4 hours before transplantation. Bone marrow was collected from the femurs and tibias of the age-matched WT male donor mice by flushing with sterile PBS. Each recipient mouse was injected with $5\times10^6$ bone marrow cells (200 μl in PBS) through the tail vein. These recipient mice were maintained under sterile SPF conditions and with antibiotic treatment (Sulfatrim at 1.6 mg/ml in drinking water) for 4 weeks to allow recovery from the irradiation. Then, these mice were received a single injection of adeno-associated virus vector ($1\times10^{11}$) expressing human D374Y-PCSK9 (rAAV8-D374Y-hPCSK9) followed by a HFD challenge for 12 weeks to induce atherosclerosis.[31]

## Monocyte-endothelial cell adhesion assay

THP-1 cells (ATCC, TIB-202) were labeled with 2.5 μM calcein AM (Sigma, C1359), or CM-DiI (ThermoFisher Scientific, V22888) in a 37 °C 5% $CO_2$ incubator for 30 minutes. The labeled cells were washed with 10 ml of PBS for 3 times to remove the residual calcein AM. After the final wash, the cells were gently resuspended at a final concentration of $1\times10^6$ cells/ml in culture medium. Calcein AM-labeled THP-1 cells ($1 \times 10^6$) were added to a confluent monolayer of primary cultured ECs, which were treated with vehicle or 20 ng/ml of TNF-α (Sigma, GF023) for 24 hours. CM-DiI-labeled THP-1 cells ($1 \times 10^6$) were added to a confluent monolayer of HUVECs, which were transduced with an adenovirus expressing GFP (Ad-GFP), RGC-32 shRNA (Ad-shRGC32), or RGC-32 cDNA (Ad-RGC32). Ad-RGC32 was constructed previously.[32] The target sequence of shRGC32 is 5′-GAT TCA CTT TAT AGG AAC AGC TT-3′. Ad-shRGC32 was generated as previously described.[32] After incubation in a 37 °C 5% $CO_2$ incubator for 1 hour, the cells were gently washed with PBS for three times, and the number of adherent calcein AM-labeled (green fluorescent signal), or CM-DiI-labeled (red fluorescent signal) THP-1 cells were determined under a Nikon fluorescence microscope. Measurements were carried out for at least 10 different view fields.

## Luciferase activity

The human ICAM-1 promoter DNA fragments from −500 to +45 bp and VCAM-1 promoter DNA fragments from −504 to +45 bp relative to the mapped transcription start sites were obtained by PCR amplification from human genomic DNA using primers containing

restriction enzyme sites for *KpnI* or *XhoI*. The primers used are listed in Online Table II. The PCR fragments were digested with restriction enzymes and cloned into the pGL4 vector. Transient transfection and luciferase assay were performed as described previously.[24] Briefly, HUVECs were transduced with Ad-GFP, Ad-shRGC32, or Ad-RGC32. 24 hours later, ICAM-1 or VCAM-1 promoter construct was transfected into the cells with Lipofectamine LTX (Invitrogen, 15338100) for 48 hours followed by the treatment with vehicle or 20 ng/ml of TNF-α for 48 hours. Luciferase activities were measured using the Dual-Luciferase reporter assay system (Promega, E1960). For each sample, a *Renilla* luciferase vector was co-transfected as an internal control, and promoter activities were normalized accordingly.

### Co-immunoprecipitation (CoIP) Assay

CoIP assay was performed as described previously.[33] In brief, HUVECs were transduced with Ad-GFP, Ad-shRGC32, or Ad-RGC32 for 48 hours, followed by vehicle or 20 ng/ml of TNF-α treatment for 6 hours. Cells were then lysed with ice-cold lysis buffer containing protease inhibitor mix (Thermo Scientific, 78430). The lysates were incubated with immunoglobulin G (IgG, Santa Cruz Biotechnology, sc-2027), RGC-32, or NF-κB p65 (Cell Signaling Technology) antibodies at 4 °C overnight by following the instruction provided in the CoIP kit (Thermo Scientific, 26149). The immunoprecipitates were pelleted, washed, and subjected to immunoblotting using RGC-32 or NF-κB p65 antibody.

### Chromatin immunoprecipitation (ChIP)

ChIP assays were performed using a ChIP assay kit (Millipore, 17-295) as described previously.[24] Briefly, HUVECs were transduced with Ad-GFP, Ad-shRGC32, or Ad-RGC32 for 48 hours, followed by vehicle or TNF-α (20 ng/ml) treatment for 6 hours. Cross-linking with 1% formaldehyde was performed at 37 °C for 10 minutes. The cells were washed twice by PBS and lysed in the lysis buffer at 4 °C for 1 hour and sonicated. The sonicated cells were centrifuged at 13,000 g for 10 minutes at 4 °C, and the supernatants were diluted using the dilution buffer. After protein measurement, equal amount of proteins was used as input control or for immunoprecipitation with NF-κB p65, RGC-32 antibody or normal rabbit IgG at 4 °C overnight. Protein A-agarose beads were added and incubated at 4 °C for 1 hour. Then, the beads were washed, and samples were eluted with elution buffer. The samples were incubated at 65 °C for 4 hours to reverse the cross-linking, and the DNA was extracted with phenol/chloroform and used for semi-quantitative and quantitative PCR. Primers for amplifying the ICAM-1 promoter were designed between −146 and −265 bp spanning the NF-κB element. For the VCAM-1 promoter, primers were designed to amplify the region between −160 and the transcription start site spanning the NF-κB element. Primers used in ChIP assays are listed in Online Table III.

### Data Analysis

All values are expressed as the mean ± SEM. For statistical analysis, two groups were compared using two-tailed Student's *t* tests (Figure 2B, 2D, 2F, 2H, 3B, 3D, 4B, 4D, 4F, 5B, 5D, and online Figure II, III, IV, VI and VII), and three groups were evaluated by one-way analysis of variance followed by Tukey's multiple comparisons (Figure 1B, 1D, 5K, and online Figure V). Four groups were evaluated by two-way analysis of variance followed by

Bonferroni post hoc tests for multiple comparisons (Figure 5E, 5G, 5I and 6B–6H) using GraphPad Prism 5.0 software. Data were considered statistically significant if $p$ value was less than 0.05.

## Results

### RGC-32 was mainly expressed in ECs of atherosclerotic lesions

To detect RGC-32 expression in human normal vessel and atherosclerotic lesions, we performed immunohistochemistry staining with RGC-32 antibody or normal rabbit IgG (negative control). RGC-32 was undetectable in human normal vessel, but it was significantly induced in the early stage and highly upregulated in advanced stage of atherosclerotic lesions (Figure 1A–1B). Immunostaining of the aortic roots of wild type (WT) and ApoE$^{-/-}$ mice fed with normal chow or HFD for 12 weeks with RGC-32 antibody or normal rabbit IgG (negative control) showed results similar to the human vessels. Although no detectable RGC-32 was observed in the aortic roots from WT and ApoE$^{-/-}$ mice fed with normal chow that had no atherosclerotic lesions, it was induced in aortic roots from ApoE$^{-/-}$ mice fed with HFD (Figure 1C–1D). Interestingly, RGC-32 expression was predominantly located in the inner layer of the vessel with the atherosclerotic lesions, suggesting that RGC-32 was expressed in ECs. To confirm this, we performed a co-immunostaining of RGC-32 with EC marker CD31, SMC marker α-SMA, or corresponding normal IgG (negative controls). As shown in Figure 1E, RGC-32 was co-localized with CD31, but not α-SMA (Online Figure I), indicating that RGC-32 was primarily expressed in ECs of the atherosclerotic lesions, which may be important for the development of atherosclerosis.

### RGC-32 deficiency attenuated atherosclerotic lesion development

To determine if RGC-32 plays a role in the development of atherosclerosis, we generated ApoE$^{-/-}$Rgc32$^{-/-}$ double knockout mice. These mice were fed HFD for 12 weeks or chow diet for one year. Oil Red O staining was performed to detect the atherosclerotic lesion formation in aortas and aortic roots. As shown in Figure 2A–2D, the area of atherosclerotic lesions seen in ApoE$^{-/-}$Rgc32$^{-/-}$ mice was significantly smaller than that in ApoE$^{-/-}$ mice. Rgc32$^{-/-}$ also reduced the size of the spontaneously developed atherosclerotic lesion in the one-year-old ApoE$^{-/-}$ mice fed with chow diet (Figure 2E–2H). Since blood lipoproteins, in particular LDL and HDL, are critical for the development of atherosclerosis,[34, 35] we tested whether Rgc32$^{-/-}$ inhibited atherosclerosis through changing the lipoprotein levels. Thus, serum isolated from ApoE$^{-/-}$ and ApoE$^{-/-}$Rgc32$^{-/-}$ mice were subjected to lipoprotein profiling. However, no significant difference in any fraction of serum lipoproteins, triglyceride, or body weight was observed between these two groups (Online Figure IIA-IIC). Liver steatosis is also highly associated with atherosclerosis.[36] However, Oil Red O staining of liver tissues and liver triglyceride assay showed that there was no difference of lipid deposition in the liver between ApoE$^{-/-}$ and ApoE$^{-/-}$Rgc32$^{-/-}$ mice (Online Figure IID-IIF).

### RGC-32 deficiency attenuated macrophage infiltration in atherosclerotic lesions

The progression of atherosclerosis involves macrophage infiltration and accumulation in the intimal plaque region.[4] Disruption of the SMC layer in the media has been observed in large mouse aortic root lesions, along with the appearance of SMCs forming the fibrous cap.[37] Therefore, to gain further insight into the differences in atherosclerosis between $ApoE^{-/-}$ and $ApoE^{-/-}Rgc32^{-/-}$ mice, we analyzed the cellular composition of the atherosclerotic lesions. Interestingly, no significant difference in the collagen and SMC content in the lesion was observed between $ApoE^{-/-}$ and $ApoE^{-/-}Rgc32^{-/-}$ mice (Figure 3A–3B). Thickness of the fibrous cap appeared not to be affected by $Rgc32^{-/-}$ as well (Figure 3A–3B). However, the macrophage content in the lesion significantly decreased in $ApoE^{-/-}Rgc32^{-/-}$ mice relative to $ApoE^{-/-}$ mice (Figure 3A–3B). Monocyte adhesion and infiltration in the early stage and proliferation of local macrophages in the established lesions contribute to lesional macrophage accumulation.[38] Co-immunofluorescent staining of macrophage marker CD68 and proliferation marker Ki67 showed that $Rgc32^{-/-}$ had no effect on the lesional macrophage proliferation (Figure 3C–3D), suggesting that the decreased macrophage content may be due to a suppression of monocyte adhesion and infiltration.

### Resident vascular cell RGC-32 was essential for atherosclerosis development

Since ECs are the primary cells that express RGC-32 in atherosclerotic lesions (Figure 1), we sought to determine if RGC-32 in resident vascular cells such as ECs contributed to the atherosclerosis development. Thus, we transplanted bone marrow (BM) cells of WT mice to the WT or $Rgc32^{-/-}$ recipient mice. These mice were then received a single injection of AAV-PCSK9 followed by a HFD challenge for 12 weeks to induce atherosclerosis.[31] PCSK9 is an enzyme that can bind to the receptor for LDL, induce its degradation, and will eventually lead to hypercholesterolemia. We used AAV-PCSK9 injection instead of $ApoE^{-/-}$ mice in order to prevent the effects of hypercholesterolemia on vascular inflammation and lesion development before BM transplantation. $ApoE^{-/-}$ mice develop atherosclerosis spontaneously due to the hypercholesterolemia, and this may obscure the potential role of macrophage RGC-32 in the early stage of atherosclerosis before the BM transplantation. En face analysis and aortic root Oil Red O staining of aorta and aortic roots showed that reconstitution of macrophage RGC-32 did not alter the function of Rgc32−/− in reducing the lesion area. As a result, significant reduced lesion area was detected in $Rgc32^{-/-}$ recipients compared to the WT recipients (Figure 4A–4D). Macrophage accumulation in $Rgc32^{-/-}$ recipients was also decreased compared with WT controls (Figure 4E–4F), similar to what was observed in $ApoE^{-/-}Rgc32^{-/-}$ mice. Moreover, WT and $Rgc32^{-/-}$ recipient mice had comparable serum PCSK9, triglyceride and cholesterol concentrations (Online Figure IIIA-IIIC). Liver steatosis also had no difference between WT and $Rgc32^{-/-}$ groups (Online Figure IIID-IIIF). These results indicate that resident vascular cell RGC-32, but not macrophage RGC-32, is essential for the atherosclerosis development.

### RGC-32 deficiency inhibited endothelial ICAM-1 and VCAM-1 expression both *in vivo* and *in vitro*

Monocyte adhesion to ECs is one of the earliest cellular events in atherosclerosis development. The oxidized lipids or proinflammatory stimuli such as TNF-α activate ECs,

which express ICAM-1, VCAM-1, and/or P-selectin attracting monocyte migration into the subendothelial space. Monocytes then differentiate into macrophages and phagocytize lipids, eventually becoming lipid-laden foam cells.[3–6] To explore the mechanism by which Rgc32$^{-/-}$ attenuated the macrophage infiltration and atherosclerosis development, we cultured the primary mouse aortic ECs from WT and Rgc32$^{-/-}$ mice and detected the expression of adhesion molecules. Interestingly, Rgc32$^{-/-}$ inhibited the expression of endothelial ICAM-1 and VCAM-1, but not P-selectin (Figure 5A–5B). To confirm the effect of Rgc32$^{-/-}$ on endothelial ICAM-1 and VCAM-1 expression *in vivo*, we immunostained the atherosclerotic lesion with ICAM-1, VCAM-1 antibody or normal rabbit IgG (negative control). As shown in Figure 5C–5D, endothelial ICAM-1 and VCAM-1 was significantly decreased in ApoE$^{-/-}$Rgc32$^{-/-}$ mice compared with ApoE$^{-/-}$ mice. In addition to ECs, vascular SMCs also express the cellular adhesion molecules ICAM-1 and VCAM-1 in atherosclerosis.[39] However, Rgc32$^{-/-}$ appeared not to affect the expression of ICAM-1, VCAM-1, or P-selectin in cultured primary mouse aortic SMCs (Online Figure IV). These data suggest that RGC-32 mainly regulates endothelial ICAM-1 and VCAM-1 expression, which may mediate the adhesion of monocytes to ECs.

## RGC-32 deficiency inhibited TNF-α-induced endothelial ICAM-1 and VCAM-1 expression and monocyte-EC interaction

TNF-α plays an essential role in adhesion molecule expression and further atherosclerosis.[40] We therefore determined if RGC-32 mediates TNF-α-induced endothelial ICAM-1 and VCAM-1 expression. The human umbilical vein endothelial cells (HUVECs) were transduced with adenovirus expressing GFP (Ad-GFP), RGC-32 shRNA (Ad-shRGC32), or RGC-32 (Ad-RGC32), and then transfected with ICAM-1 or VCAM-1 promoter constructs. Luciferase activity assay was performed following vehicle or TNF-α treatment. Consistent with previous studies, TNF-α increased ICAM-1 and VCAM-1 promoter activities.[10] However, knockdown of RGC-32 diminished the TNF-α-increased promoter activities while RGC-32 overexpression enhanced the promoter activities (Figure 5E), suggesting that RGC-32 played a critical role in TNF-α-induced endothelial ICAM-1 and VCAM-1 transcription. We also confirmed the regulation of ICAM-1 and VCAM-1 by RGC-32 at protein level in primary cultured mouse aortic ECs. TNF-α significantly induced both the ICAM-1 and VCAM-1 expression in WT ECs. However, Rgc32$^{-/-}$ diminished the effect of TNF-α (Figure 5F–5G). To assess the functional significance of RGC-32 on ICAM-1 and VCAM-1 expression, we tested if RGC-32 affects the monocyte-EC interaction. To this end, primary mouse aortic ECs were treated with vehicle or TNF-α for 24 hours, and then incubated with Calcein AM-labeled THP-1 cells. As shown in Figure 5H–5I, TNF-α treatment increased the adhesion of THP-1 monocytes to WT ECs. Rgc32$^{-/-}$ attenuated THP-1 adhesion with and without TNF-α treatment. To test the direct effect of RGC-32 on monocyte-EC interaction, RGC-32 was knocked down or overexpressed in HUVECs (Online Figure V) followed by incubation with CM-DiI-labeled THP-1 cells. As shown in Figure 5J–5K, knockdown of RGC-32 suppressed while overexpression of RGC-32 enhanced the adhesion of THP-1 monocytes to HUVECs. These results indicated that RGC-32 mediates TNF-α-induced endothelial ICAM-1 and VCAM-1 expression, which further facilitates the monocyte-EC interaction.

### RGC-32 mediated endothelial ICAM-1 and VCAM-1 expression, at least partially, through NF-κB signaling

Since NF-κB is a critical transcription factor regulating endothelial ICAM-1 and VCAM-1 expression,[41, 42] we hypothesized that RGC-32 may regulate endothelial ICAM-1 and VCAM-1 expression via NF-κB signaling. To test this hypothesis, we used ammonium pyrrolidinedithiocarbamate (PDTC) to block NF-κB signaling in HUVECs with forced expression of RGC-32. As shown in Figure 6A–6B, RGC-32 overexpression induced ICAM-1 and VCAM-1 expression accompanied by an increased NF-κB phosphorylation (activation). PDTC blocked RGC-32-induced NF-κB phosphorylation as well as ICAM-1 and VCAM-1 expression (Figure 6A–6B). Consistently, knockdown of RGC-32 blocked while overexpression of RGC-32 increased TNF-α-induced NF-κB nuclear translocation (Online Figure VIA-VID). These results indicated that RGC-32 regulates endothelial ICAM-1 and VCAM-1 expression, at least partially, through NF-κB signaling pathway.

To determine how RGC-32 regulates NF-κB function, we detected if RGC-32 interacts with NF-κB. Co-immunoprecipitation assay showed that RGC-32 physically interacted with NF-κB, and TNF-α treatment significantly increased this interaction (Figure 6C–6D). Since NF-κB regulates ICAM-1 and VCAM-1 transcription by binding to their promoters, we further determined if RGC-32 affects the interaction of NF-κB with ICAM-1 and VCAM-1 promoters using a chromatin-immunoprecipitation assay. As shown in Figure 6E–6F, RGC-32 knockdown decreased while RGC-32 overexpression increased TNF-α-induced NF-κB binding to the ICAM-1 and VCAM-1 promoters. Intriguingly, TNF-α induced RGC-32 nuclear translocation (Online Figure VII), and chromatin-immunoprecipitation assay using RGC-32 antibody showed that TNF-α increased RGC-32 binding to the ICAM-1 and VCAM-1 promoters (Figure 6G–6H). Our results demonstrated that RGC-32 directly binds with NF-κB and facilitates its binding to ICAM-1 and VCAM-1 promoters, and thus promotes their expression during atherogenesis.

## Discussion

Although atherosclerosis was once considered as a lipid-storage disease, it is now recognized as a subacute inflammatory condition of the vessel wall, characterized by infiltration of macrophages and T cells, which interact with one another and with cells in the arterial wall.[43] Recent study demonstrates that RGC-32 is expressed in human atherosclerotic arterial wall.[25] However, it is unclear if RGC-32 plays a role in arterial inflammation and atherosclerosis development. Our current study demonstrates that RGC-32 is expressed strongly in ECs of both mouse and human atherosclerotic lesions (Figure 1). Interestingly, $ApoE^{-/-}Rgc32^{-/-}$ mice exhibit significantly decreased atherosclerotic lesion development compared with $ApoE^{-/-}$ control mice under both HFD and chow diet conditions (Figure 2), suggesting a critical role of RGC-32 in atherosclerosis.

The initial steps of atherosclerosis include adhesion of circulating monocytes to the ECs and migration of the adherent monocytes into the intima.[37] EC activation upon exposure to oxidized lipids and proinflammatory stimuli, such as TNF-α, induces ICAM-1 and VCAM-1 expression, mediating adhesion of monocytes to ECs.[3–6] $Rgc32^{-/-}$ significantly reduces the macrophage content in atherosclerotic lesions (Figure 3A–3B), and decreases

ICAM-1 and VCAM-1 expression in ECs (Figure 5A–5D). Rgc32$^{-/-}$ also blocks TNF-α-induced endothelial ICAM-1 and VCAM-1 expression and monocyte-EC interaction (Figure 5E–5I). In addition to ECs, vascular SMCs also express ICAM-1 and VCAM-1 in atherosclerosis.[39] Our *in vivo* data showed that ICAM-1 and VCAM-1 expression inside the lesion was decreased in ApoE$^{-/-}$Rgc32$^{-/-}$ mice compared with the ApoE$^{-/-}$ control mice (Figure 5C). However, Rgc32$^{-/-}$ appeared not to affect ICAM-1, VCAM-1, or P-selectin expression in primary cultured vascular SMCs (Online Figure IV), suggesting the reduced ICAM-1 and VCAM-1 expression in lesion SMC may be due to an indirect effect of Rgc32$^{-/-}$, e.g., the decreased macrophage infiltration. Indeed, there is a correlation between the extent of adhesion molecule expression in lesion SMC and macrophage infiltration.[39] TNF-α and IL-1β secreted by macrophages increase ICAM-1 and VCAM-1 expression in vascular SMCs.[44, 45] Moreover, the atherosclerotic lesion progression also involves the migration of SMCs from the media to the intima, proliferation of the SMCs, and increased synthesis of extracellular matrix, such as collagen.[43] However, RGC-32 appears not to alter the collagen or SMC content in atherosclerotic lesions (Figure 3A–3B), suggesting that RGC-32 play a minimal role in SMC function during atherosclerosis development.

Transcription factor NF-κB is a predominant regulator of endothelial ICAM-1 and VCAM-1 expression.[7–10] Blockade of NF-κB abolishes adhesion molecule induction in ECs, which impairs monocyte recruitment to atherosclerotic plaques.[13] However, it is largely unknown how NF-κB regulates endothelial ICAM-1 and VCAM-1 expression. The present study demonstrates that RGC-32 directly interacts with NF-κB (Figure 6C–6D) and facilitates NF-κB nuclear translocation (Online Figure VIC-VID). RGC-32 enhances TNF-α-induced NF-κB binding to ICAM-1 and VCAM-1 promoters (Figure 6E–6F), and promotes their transcription activities (Figure 5E).

Following recruitment into the arterial intima, monocytes differentiate to macrophages in which large amounts of lipid accumulate through the uptake of modified lipoproteins, resulting in foam cell formation. Macrophage-derived foam cells in turn stimulate smooth muscle cell proliferation and migration, and contribute to the progression of atherosclerosis.[46] Our previous studies have shown that macrophages with RGC-32 deficiency exhibit significant defects in phagocytosis,[47] suggesting that RGC-32 may contribute to the foam cell formation. Moreover, RGC-32 deficiency-caused decrease in NF-kB activity may protect ECs from other inflammatory responses beyond the blockade of ICAM-1 and VCAM-1 expression. Therefore, targeting RGC-32 may have better advantage than simply targeting the adhesion molecules for treating atherosclerosis.

One limitation of this study is that only male mice are used to test RGC-32 function. Sex can cause major effects on the outcome of atherosclerosis studies in both human and animal models. Indeed, atherosclerotic lesions in the aortic root are larger in female than male mice. Recently, American Heart Association have advised to include sufficient mice of both sexes in atherosclerotic studies.[48, 49] Since our completed studies were initiated several years ago, we were unable to determine the role of RGC-32 in female mice during the study. However, the sex difference is an excellent subject for the future investigation.

Taken together, our present study demonstrates that RGC-32 mediates atherogenesis in male animal model by facilitating monocyte-EC interaction, due to the induction of endothelial ICAM-1 and VCAM-1 expression, at least partially, through NF-κB signaling pathway. The selective induction in ECs and its role facilitating monocyte-EC interaction make RGC-32 as a novel potential therapeutic target for atherosclerosis.

## Supplementary Material

Refer to Web version on PubMed Central for supplementary material.

## Acknowledgments

None

**Sources of Funding:** This work was supported by grants from National Institutes of Health HL119053, HL123302, and HL135854 (to S.Y.C.) and American Heart Association Scientist Development Grant 17SDG32790003 (to X.B.C.).

## Abbreviations

| | |
|---|---|
| **ApoE** | apolipoprotein E |
| **CoIP** | Co-immunoprecipitation |
| **ECs** | endothelial cells |
| **HDL** | high-density lipoprotein |
| **HFD** | high-fat diet |
| **HUVEC** | human umbilical vein endothelial cell |
| **ICAM-1** | intercellular adhesion molecule-1 |
| **LDL** | low-density lipoprotein |
| **NF-κB** | nuclear factor-κB |
| **PDTC** | ammonium pyrrolidinedithiocarbamate |
| **RGC-32** | response gene to complement 32 |
| **SMCs** | smooth muscle cells |
| **TNF-α** | tumor necrosis factor-α |
| **VCAM-1** | vascular adhesion molecule-1 |
| **VLDL** | very low-density lipoprotein |
| **WT** | wild-type |

## References

1. Libby P. Inflammation in atherosclerosis. Nature. 2002; 420:868–874. [PubMed: 12490960]

2. Libby P. Inflammation in atherosclerosis. Arterioscler Thromb Vasc Biol. 2012; 32:2045–2051. [PubMed: 22895665]
3. Bevilacqua MP, Nelson RM, Mannori G, Cecconi O. Endothelial-leukocyte adhesion molecules in human disease. Annu Rev Med. 1994; 45:361–378. [PubMed: 7515220]
4. Moore KJ, Tabas I. Macrophages in the pathogenesis of atherosclerosis. Cell. 2011; 145:341–355. [PubMed: 21529710]
5. Moore KJ, Sheedy FJ, Fisher EA. Macrophages in atherosclerosis: A dynamic balance. Nat Rev Immunol. 2013; 13:709–721. [PubMed: 23995626]
6. Zakynthinos E, Pappa N. Inflammatory biomarkers in coronary artery disease. J Cardiol. 2009; 53:317–333. [PubMed: 19477372]
7. de Winther MP, Kanters E, Kraal G, Hofker MH. Nuclear factor kappab signaling in atherogenesis. Arterioscler Thromb Vasc Biol. 2005; 25:904–914. [PubMed: 15731497]
8. Weber C, Erl W, Pietsch A, Strobel M, Ziegler-Heitbrock HW, Weber PC. Antioxidants inhibit monocyte adhesion by suppressing nuclear factor-kappa b mobilization and induction of vascular cell adhesion molecule-1 in endothelial cells stimulated to generate radicals. Arterioscler Thromb. 1994; 14:1665–1673. [PubMed: 7522548]
9. Lu Y, Zhu X, Liang GX, Cui RR, Liu Y, Wu SS, Liang QH, Liu GY, Jiang Y, Liao XB, Xie H, Zhou HD, Wu XP, Yuan LQ, Liao EY. Apelin-apj induces icam-1, vcam-1 and mcp-1 expression via nf-kappab/jnk signal pathway in human umbilical vein endothelial cells. Amino Acids. 2012; 43:2125–2136. [PubMed: 22532031]
10. Yan S, Zhang X, Zheng H, Hu D, Zhang Y, Guan Q, Liu L, Ding Q, Li Y. Clematichinenoside inhibits vcam-1 and icam-1 expression in tnf-alpha-treated endothelial cells via nadph oxidase-dependent ikappab kinase/nf-kappab pathway. Free Radic Biol Med. 2015; 78:190–201. [PubMed: 25463279]
11. Ledebur HC, Parks TP. Transcriptional regulation of the intercellular adhesion molecule-1 gene by inflammatory cytokines in human endothelial cells. Essential roles of a variant nf-kappa b site and p65 homodimers. J Biol Chem. 1995; 270:933–943. [PubMed: 7822333]
12. Marx N, Sukhova GK, Collins T, Libby P, Plutzky J. Pparalpha activators inhibit cytokine-induced vascular cell adhesion molecule-1 expression in human endothelial cells. Circulation. 1999; 99:3125–3131. [PubMed: 10377075]
13. Gareus R, Kotsaki E, Xanthoulea S, van der Made I, Gijbels MJ, Kardakaris R, Polykratis A, Kollias G, de Winther MP, Pasparakis M. Endothelial cell-specific nf-kappab inhibition protects mice from atherosclerosis. Cell Metab. 2008; 8:372–383. [PubMed: 19046569]
14. Badea T, Niculescu F, Soane L, Fosbrink M, Sorana H, Rus V, Shin ML, Rus H. Rgc-32 increases p34cdc2 kinase activity and entry of aortic smooth muscle cells into s-phase. J Biol Chem. 2002; 277:502–508. [PubMed: 11687586]
15. Fosbrink M, Cudrici C, Tegla CA, Soloviova K, Ito T, Vlaicu S, Rus V, Niculescu F, Rus H. Response gene to complement 32 is required for c5b-9 induced cell cycle activation in endothelial cells. Exp Mol Pathol. 2009; 86:87–94. [PubMed: 19162005]
16. Li F, Luo Z, Huang W, Lu Q, Wilcox CS, Jose PA, Chen S. Response gene to complement 32, a novel regulator for transforming growth factor-beta-induced smooth muscle differentiation of neural crest cells. J Biol Chem. 2007; 282:10133–10137. [PubMed: 17327222]
17. Fosbrink M, Cudrici C, Niculescu F, Badea TC, David S, Shamsuddin A, Shin ML, Rus H. Overexpression of rgc-32 in colon cancer and other tumors. Exp Mol Pathol. 2005; 78:116–122. [PubMed: 15713436]
18. Vlaicu SI, Tegla CA, Cudrici CD, Fosbrink M, Nguyen V, Azimzadeh P, Rus V, Chen H, Mircea PA, Shamsuddin A, Rus H. Epigenetic modifications induced by rgc-32 in colon cancer. Exp Mol Pathol. 2010; 88:67–76. [PubMed: 19883641]
19. Kim DS, Lee JY, Lee SM, Choi JE, Cho S, Park JY. Promoter methylation of the rgc32 gene in nonsmall cell lung cancer. Cancer. 2011; 117:590–596. [PubMed: 20862745]
20. Saigusa K, Imoto I, Tanikawa C, Aoyagi M, Ohno K, Nakamura Y, Inazawa J. Rgc32, a novel p53-inducible gene, is located on centrosomes during mitosis and results in g2/m arrest. Oncogene. 2007; 26:1110–1121. [PubMed: 17146433]

21. Huang WY, Li ZG, Rus H, Wang X, Jose PA, Chen SY. Rgc-32 mediates transforming growth factor-beta-induced epithelial-mesenchymal transition in human renal proximal tubular cells. J Biol Chem. 2009; 284:9426–9432. [PubMed: 19158077]
22. Guo X, Jose PA, Chen SY. Response gene to complement 32 interacts with smad3 to promote epithelial-mesenchymal transition of human renal tubular cells. Am J Physiol Cell Physiol. 2011; 300:C1415–1421. [PubMed: 21307346]
23. Cui XB, Luan JN, Ye J, Chen SY. Rgc32 deficiency protects against high-fat diet-induced obesity and insulin resistance in mice. J Endocrinol. 2015; 224:127–137. [PubMed: 25385871]
24. Cui XB, Luan JN, Chen SY. Rgc-32 deficiency protects against hepatic steatosis by reducing lipogenesis. J Biol Chem. 2015; 290:20387–20395. [PubMed: 26134570]
25. Vlaicu SI, Tatomir A, Boodhoo D, Ito T, Fosbrink M, Cudrici C, Mekala AP, Ciriello J, Crisan D, Botan E, Rus V, Rus H. Rgc-32 is expressed in the human atherosclerotic arterial wall: Role in c5b-9-induced cell proliferation and migration. Exp Mol Pathol. 2016; 101:221–230. [PubMed: 27619159]
26. Cui XB, Guo X, Chen SY. Response gene to complement 32 deficiency causes impaired placental angiogenesis in mice. Cardiovasc Res. 2013; 99:632–639. [PubMed: 23695833]
27. Mehlem A, Hagberg CE, Muhl L, Eriksson U, Falkevall A. Imaging of neutral lipids by oil red o for analyzing the metabolic status in health and disease. Nat Protoc. 2013; 8:1149–1154. [PubMed: 23702831]
28. Kobayashi M, Inoue K, Warabi E, Minami T, Kodama T. A simple method of isolating mouse aortic endothelial cells. J Atheroscler Thromb. 2005; 12:138–142. [PubMed: 16020913]
29. Golovina VA, Blaustein MP. Preparation of primary cultured mesenteric artery smooth muscle cells for fluorescent imaging and physiological studies. Nat Protoc. 2006; 1:2681–2687. [PubMed: 17406524]
30. Dutta P, Hoyer FF, Sun Y, Iwamoto Y, Tricot B, Weissleder R, Magnani JL, Swirski FK, Nahrendorf M. E-selectin inhibition mitigates splenic hsc activation and myelopoiesis in hypercholesterolemic mice with myocardial infarction. Arterioscler Thromb Vasc Biol. 2016; 36:1802–1808. [PubMed: 27470513]
31. Bjorklund MM, Hollensen AK, Hagensen MK, Dagnaes-Hansen F, Christoffersen C, Mikkelsen JG, Bentzon JF. Induction of atherosclerosis in mice and hamsters without germline genetic engineering. Circ Res. 2014; 114:1684–1689. [PubMed: 24677271]
32. Wang JN, Shi N, Xie WB, Guo X, Chen SY. Response gene to complement 32 promotes vascular lesion formation through stimulation of smooth muscle cell proliferation and migration. Arterioscler Thromb Vasc Biol. 2011; 31:e19–26. [PubMed: 21636805]
33. Xie WB, Li Z, Shi N, Guo X, Tang J, Ju W, Han J, Liu T, Bottinger EP, Chai Y, Jose PA, Chen SY. Smad2 and myocardin-related transcription factor b cooperatively regulate vascular smooth muscle differentiation from neural crest cells. Circ Res. 2013; 113:e76–86. [PubMed: 23817199]
34. Badimon L, Vilahur G. Ldl-cholesterol versus hdl-cholesterol in the atherosclerotic plaque: Inflammatory resolution versus thrombotic chaos. Ann N Y Acad Sci. 2012; 1254:18–32. [PubMed: 22548566]
35. Assmann G, Gotto AM Jr. Hdl cholesterol and protective factors in atherosclerosis. Circulation. 2004; 109:III8–14. [PubMed: 15198960]
36. Xu X, Lu L, Dong Q, Li X, Zhang N, Xin Y, Xuan S. Research advances in the relationship between nonalcoholic fatty liver disease and atherosclerosis. Lipids Health Dis. 2015; 14:158. [PubMed: 26631018]
37. Libby P, Ridker PM, Hansson GK. Progress and challenges in translating the biology of atherosclerosis. Nature. 2011; 473:317–325. [PubMed: 21593864]
38. Robbins CS, Hilgendorf I, Weber GF, et al. Local proliferation dominates lesional macrophage accumulation in atherosclerosis. Nat Med. 2013; 19:1166–1172. [PubMed: 23933982]
39. Braun M, Pietsch P, Schror K, Baumann G, Felix SB. Cellular adhesion molecules on vascular smooth muscle cells. Cardiovasc Res. 1999; 41:395–401. [PubMed: 10341839]
40. Chang CC, Chu CF, Wang CN, Wu HT, Bi KW, Pang JH, Huang ST. The anti-atherosclerotic effect of tanshinone iia is associated with the inhibition of tnf-alpha-induced vcam-1, icam-1 and cx3cl1 expression. Phytomedicine. 2013

41. Iademarco MF, McQuillan JJ, Rosen GD, Dean DC. Characterization of the promoter for vascular cell adhesion molecule-1 (vcam-1). J Biol Chem. 1992; 267:16323–16329. [PubMed: 1379595]
42. Chen CC, Rosenbloom CL, Anderson DC, Manning AM. Selective inhibition of e-selectin, vascular cell adhesion molecule-1, and intercellular adhesion molecule-1 expression by inhibitors of i kappa b-alpha phosphorylation. J Immunol. 1995; 155:3538–3545. [PubMed: 7561050]
43. Rocha VZ, Libby P. Obesity, inflammation, and atherosclerosis. Nat Rev Cardiol. 2009; 6:399–409. [PubMed: 19399028]
44. Thorne SA, Abbot SE, Stevens CR, Winyard PG, Mills PG, Blake DR. Modified low density lipoprotein and cytokines mediate monocyte adhesion to smooth muscle cells. Atherosclerosis. 1996; 127:167–176. [PubMed: 9125306]
45. Braun M, Pietsch P, Felix SB, Baumann G. Modulation of intercellular adhesion molecule-1 and vascular cell adhesion molecule-1 on human coronary smooth muscle cells by cytokines. J Mol Cell Cardiol. 1995; 27:2571–2579. [PubMed: 8825878]
46. Schrijvers DM, De Meyer GR, Herman AG, Martinet W. Phagocytosis in atherosclerosis: Molecular mechanisms and implications for plaque progression and stability. Cardiovasc Res. 2007; 73:470–480. [PubMed: 17084825]
47. Tang R, Zhang G, Chen SY. Response gene to complement 32 protein promotes macrophage phagocytosis via activation of protein kinase c pathway. J Biol Chem. 2014; 289:22715–22722. [PubMed: 24973210]
48. Daugherty A, Tall AR, Daemen M, Falk E, Fisher EA, Garcia-Cardena G, Lusis AJ, Owens AP 3rd, Rosenfeld ME, Virmani R, American Heart Association Council on Arteriosclerosis T, Vascular B, Council on Basic Cardiovascular S. Recommendation on design, execution, and reporting of animal atherosclerosis studies: A scientific statement from the american heart association. Arterioscler Thromb Vasc Biol. 2017
49. Robinet P, Milewicz DM, Cassis LA, Leeper NJ, Lu HS, Smith JD. Consideration of sex differences in design and reporting of experimental arterial pathology studies-statement from atvb council. Arterioscler Thromb Vasc Biol. 2018

## Highlights

- Response gene to complement 32 (RGC-32) is induced in endothelial cells of atherosclerotic lesions.
- Endothelial RGC-32 promotes atherosclerosis through mediating TNF-α-induced intercellular cell adhesion molecule-1 (ICAM-1) and vascular cell adhesion molecule-1 (VCAM-1) expression and monocyte-endothelium interaction.
- RGC-32 mediates TNF-α-induced endothelial ICAM-1 and VCAM-1 expression via directly interacting with nuclear factor (NF)-κB and facilitating its nuclear translocation and binding to the ICAM-1 and VCAM-1 promoter regions.
- Our findings provide a rationale to target endothelial RGC-32 as a new therapeutic strategy to prevent atherosclerosis.

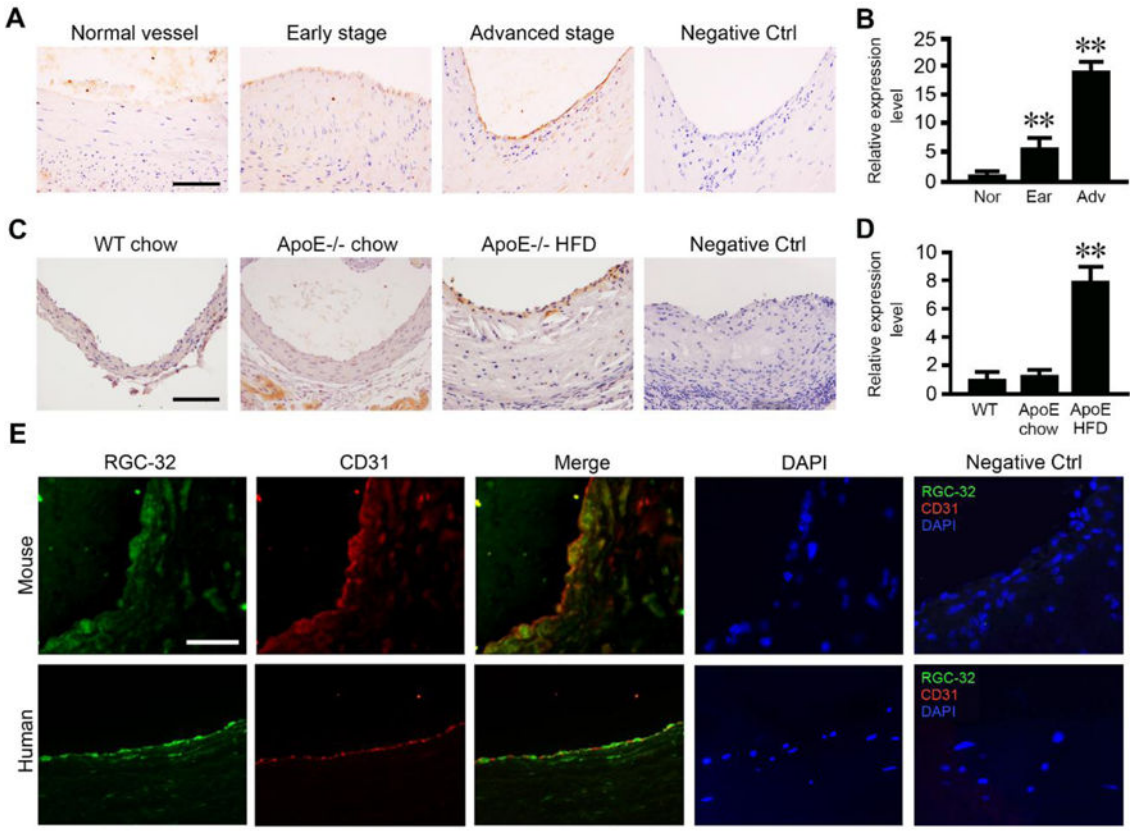


**Figure 1. RGC-32 expression was induced in ECs of atherosclerotic lesions**

**A**, Representative images of immunohistochemistry staining for RGC-32 in human normal vessel as well as early and advanced stage atherosclerotic lesions. Negative control was stained with normal rabbit IgG. Scale bar: 200 μm. **B**, Quantification of RGC-32 expression shown in A. ***P*<0.01 compared with normal vessel groups (n=3). Nor: normal vessel; Ear: early stage; Adv: advanced stage. **C**, Representative images of immunohistochemistry staining for RGC-32 in aortic roots of wild-type (WT) and ApoE$^{-/-}$ mice fed with chow or high-fat diet (HFD) for 12 weeks. Negative control was stained with normal rabbit IgG. Scale bar: 200 μm. **D**, Quantification of RGC-32 expression shown in B. ***P*<0.01 compared with ApoE$^{-/-}$ chow groups (n=6). **E**, Representative images of immunofluorescent staining for RGC-32 (green), CD31 (red, ECs), and 4′,6-diamidino-2-phenylindole (DAPI, blue, nuclei) in aortic roots of the ApoE$^{-/-}$ mice fed with HFD for 12 weeks (n=6) as well as in advanced human atherosclerotic lesions (n=3). Negative control was stained with normal IgG. Scale bar: 100 μm.

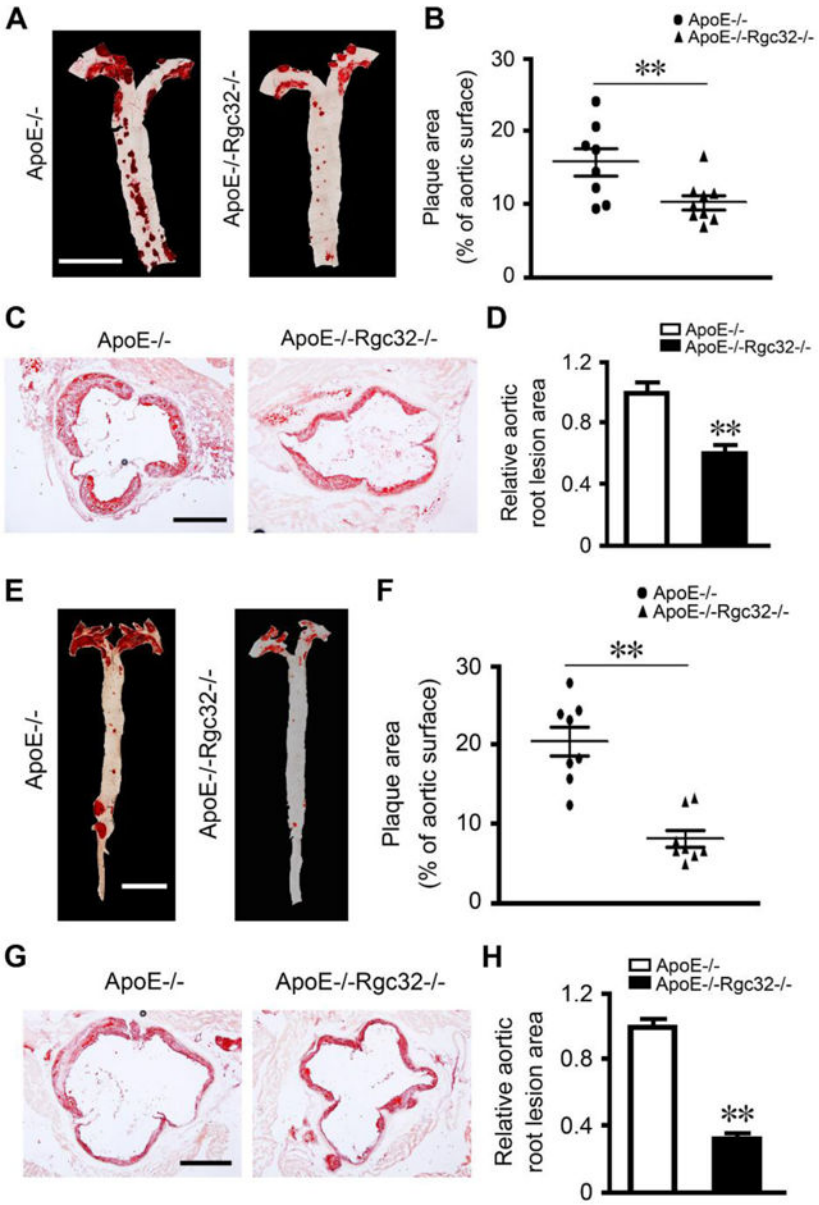


**Figure 2. RGC-32 deficiency attenuated diet-induced atherosclerosis in ApoE$^{-/-}$ mice**

**A-D**, ApoE$^{-/-}$ (n=8) and ApoE$^{-/-}$Rgc32$^{-/-}$ (n=9) mice were fed with high-fat diet (HFD) for 12 weeks. **A**, Representative images of en face Oil Red O staining of the aortas. Scale bar: 0.5 cm. **B**, Quantification of the atherosclerotic lesions in en face aortas shown in A, which was expressed as percentage of lesions relative to total aortic area. **C**, Representative Oil Red O staining of aortic root. **D**, Quantification of aortic root lesion by measuring the Oil Red O-positive area. Scale bar: 500 μm. ** $P$<0.01 compared with ApoE$^{-/-}$ groups (n=8-9). **E-H**, ApoE$^{-/-}$ (n=8) and ApoE$^{-/-}$Rgc32$^{-/-}$ (n=8) mice were fed with chow diet for one year. **E**, Representative images of en face Oil Red O staining of the aortas. Scale bar: 0.5 cm. **F**, Quantification of the atherosclerotic lesions in en face aortas in E and shown as the percentage of lesions relative to total aortic area. **G**, Representative Oil Red O staining of the

aortic root. **H**, Quantification of aortic root lesion by the Oil Red O-positive area. Scale bar: 500 μm. ** $P<0.01$ compared with $ApoE^{-/-}$ groups (n=8).

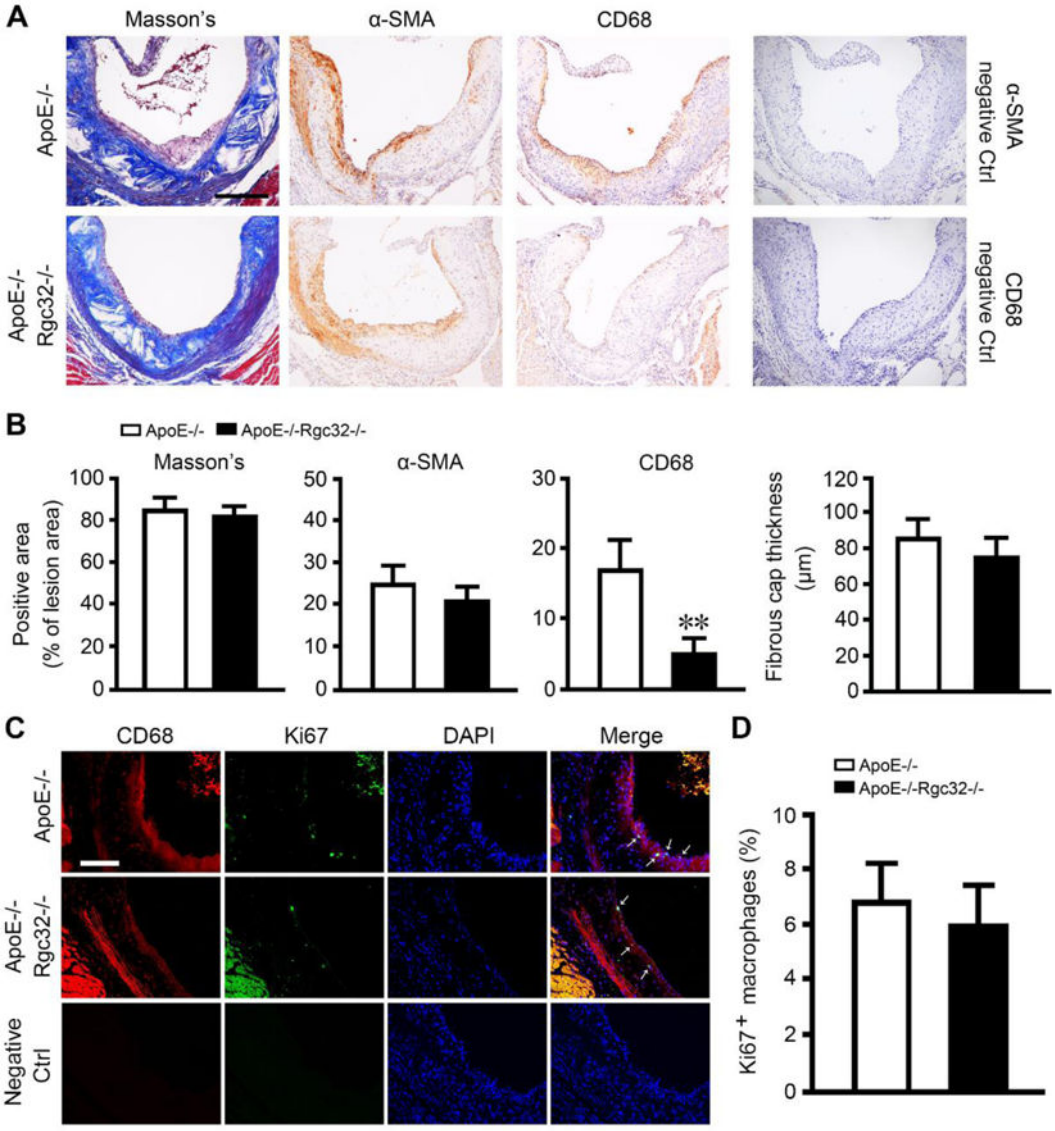


**Figure 3. RGC-32 deficiency inhibited macrophage content in atherosclerotic lesions**

$ApoE^{-/-}$ (n=8) and $ApoE^{-/-}Rgc32^{-/-}$ (n=9) mice were fed high-fat diet (HFD) for 12 weeks. **A**, Representative images of Masson's staining for collagen content and immunohistochemistry staining for SMC content (α-smooth muscle actin, α-SMA) or macrophage accumulation (CD68). Staining with corresponding normal IgG was used as negative control. Scale bar: 200 μm. **B**, Quantitative analysis of collagen deposition, α-SMA- or CD68-positive area, and fibrous cap thickness as indicated. $^{**}P<0.01$ compared with $ApoE^{-/-}$ groups (n=8-9). **C**, Representative images of immunofluorescent staining for CD68 (Red, macrophages), Ki67 (green), and 4′,6-diamidino-2-phenylindole (DAPI, blue, nuclei) in aortic roots of the $ApoE^{-/-}$ (n=8) and $ApoE^{-/-}Rgc32^{-/-}$ (n=9) mice fed HFD for 12 weeks. Staining with corresponding normal IgG was used as negative controls. **D**, Quantification of the Ki67 staining of CD68-positive cells in C and shown as the percentage of the total CD68-positive cells. Scale bar: 100 μm.

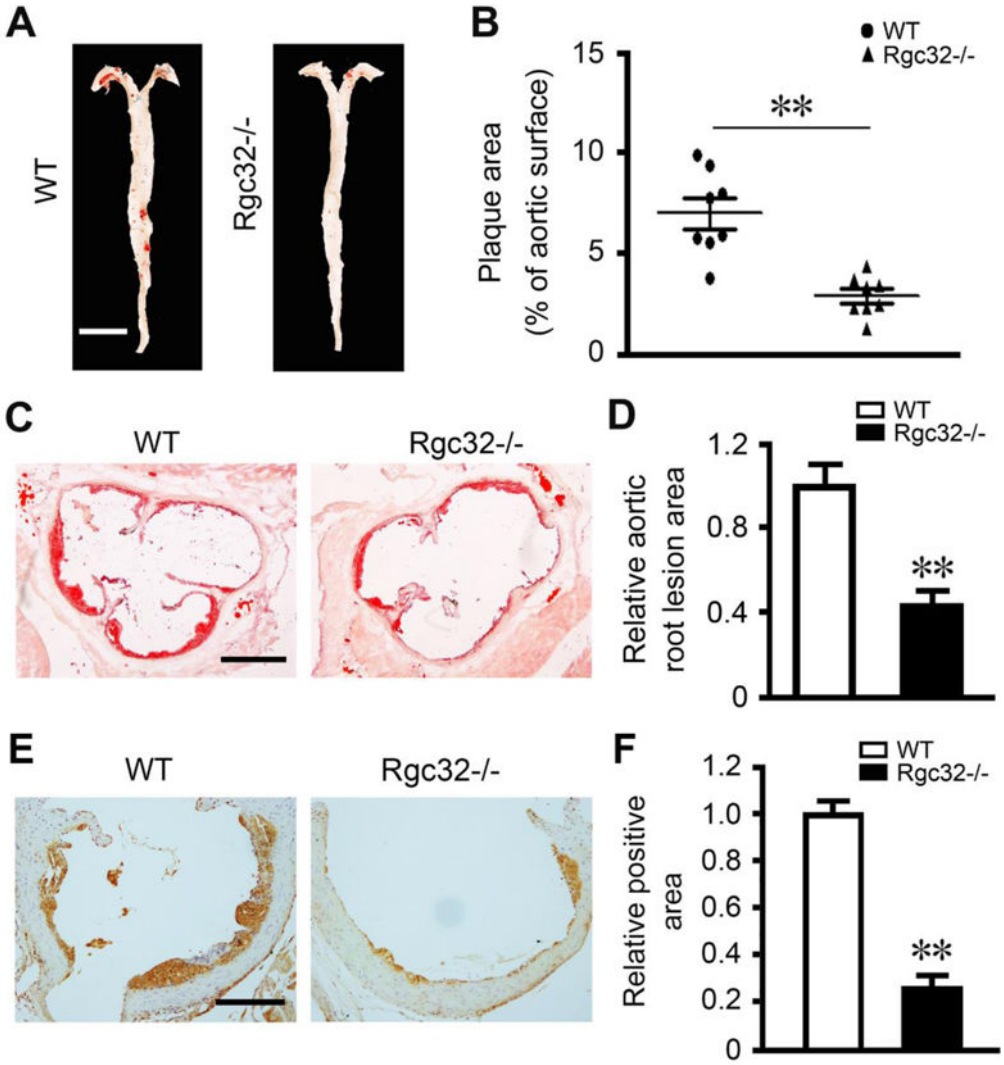


**Figure 4. Resident vascular cell RGC-32 was essential for atherosclerosis development**

Wild-type (WT) (n=8) or Rgc32$^{-/-}$ (n=8) recipient mice were transplanted with bone marrow from WT mice. These mice were then received a single injection of AAV-PCSK9 and fed high-fat diet (HFD) for 12 weeks. **A**, Representative images of en face Oil Red O staining of the aortas. Scale bar: 0.5 cm. **B**, Quantification of the atherosclerotic lesions in en face aortas shown in A, which was expressed as percentage of lesions relative to total aortic area. **C**, Representative Oil Red O staining of aortic root. Scale bar: 500 μm. **D**, Quantification of aortic root lesion by measuring the Oil Red O-positive area. $^{**}P<0.01$ compared with WT groups (n=8). **E**, Representative images of immunohistochemistry staining for macrophage accumulation (CD68) in aortic roots. Scale bar: 200 μm. **F**, Quantitative analysis of CD68-positive area shown in E. $^{**}P<0.01$ compared with WT groups (n=8).

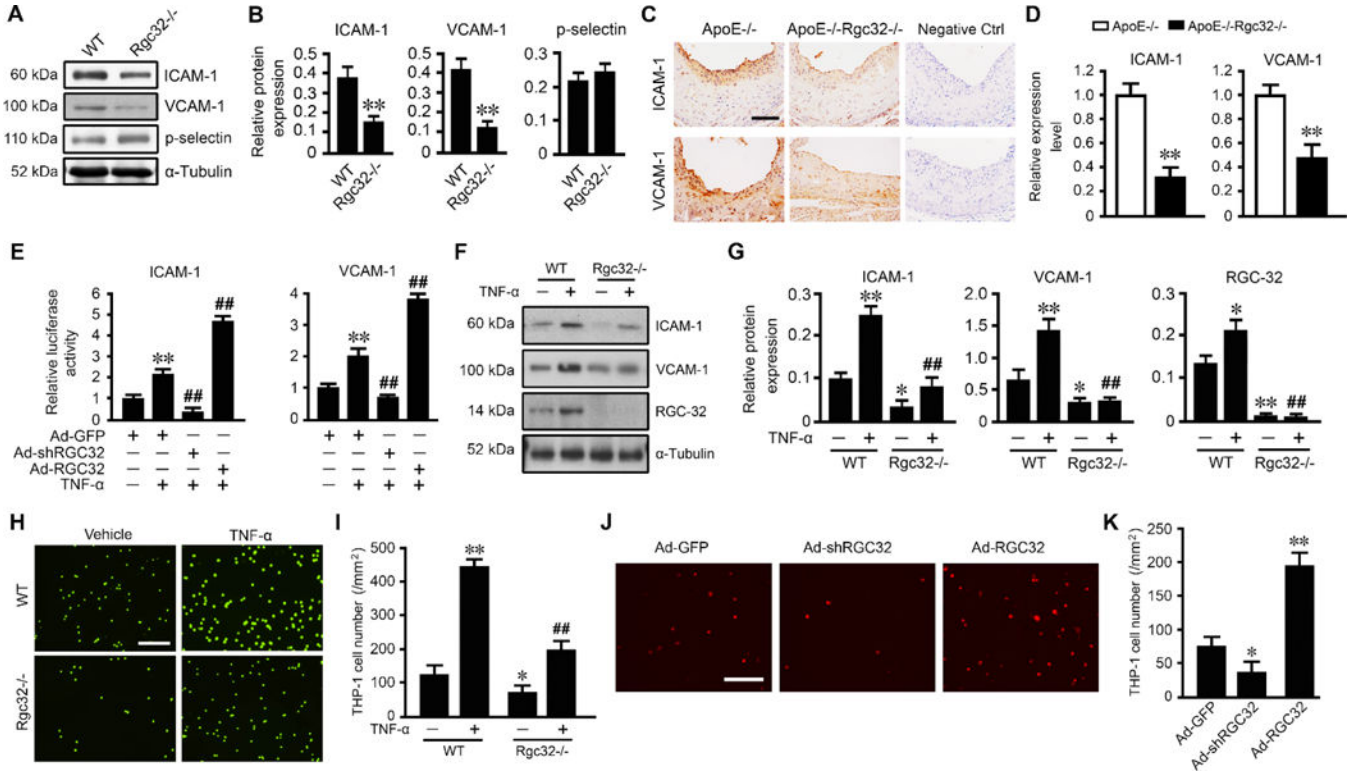


**Figure 5. RGC-32 was essential for TNF-α-induced endothelial ICAM-1 and VCAM-1 expression and monocyte-EC interaction**

**A-B**,ICAM-1, VCAM-1, and p-selectin protein expression in primary mouse aortic ECs from wild-type (WT) and Rgc32$^{-/-}$ mice was detected by Western blot and normalized to α-tubulin level. ***P*<0.01 compared with WT groups (n=3). **C-D**, Representative immunohistochemistry staining and quantification of ICAM-1 and VCAM-1 in the intima layer of the aortic roots of ApoE$^{-/-}$ (n=8) and ApoE$^{-/-}$Rgc32$^{-/-}$ (n=9) mice fed high-fat diet (HFD) for 12 weeks. Staining with corresponding normal IgG served as as negative controls. ***P*<0.01 compared with ApoE$^{-/-}$ groups (n=8-9). Scale bar: 100 μm. **E**, HUVECs were transduced with Ad-GFP, Ad-shRGC32, or Ad-RGC32 for 24 hours, followed by transfection of ICAM-1 or VCAM-1 promoter construct and treatment with vehicle or 20 ng/ml TNF-α for 48 hours. Luciferase assay was then performed, and luciferase activity was normalized to *Renilla* activity. ***P*<0.01 compared with Ad-GFP groups; $^{\#\#}$*P*<0.01 compared with Ad-GFP groups treated with TNF-α; n=3. **F-G**, Primary mouse aortic ECs from WT and Rgc32$^{-/-}$ mice were treated with vehicle or 20 ng/ml of TNF-α for 24 hours. ICAM-1, VCAM-1 and RGC-32 protein expression was detected by Western blot and normalized to α-tubulin level. **P*<0.05, ***P*<0.01 compared with WT groups treated with vehicle (−); $^{\#\#}$*P*<0.01 compared with WT groups treated with TNF-α; n=6. **H-I**, WT and Rgc32$^{-/-}$ primary mouse aortic EC monolayer was treated with vehicle or TNF-α for 24 hours followed by incubation with calcein AM-labeled (green) THP-1 cells. After washing by PBS, the number of the adherent THP-1 cells in 10 random fields was counted. **P*<0.05, ***P*<0.01 compared with WT groups treated with vehicle (−); $^{\#\#}$*P*<0.01 compared with WT groups treated with TNF-α; n=3. **J-K**, HUVECs were transduced with Ad-GFP, Ad-shRGC32, or Ad-RGC32 for 48 hours followed by incubation with CM-DiI-labeled (Red)

THP-1 cells. After washing by PBS, the number of the adherent THP-1 cells in 10 random fields was counted. *$P$<0.05, **$P$<0.01 compared with Ad-GFP groups (n=3). Scale bar: 100 μm.

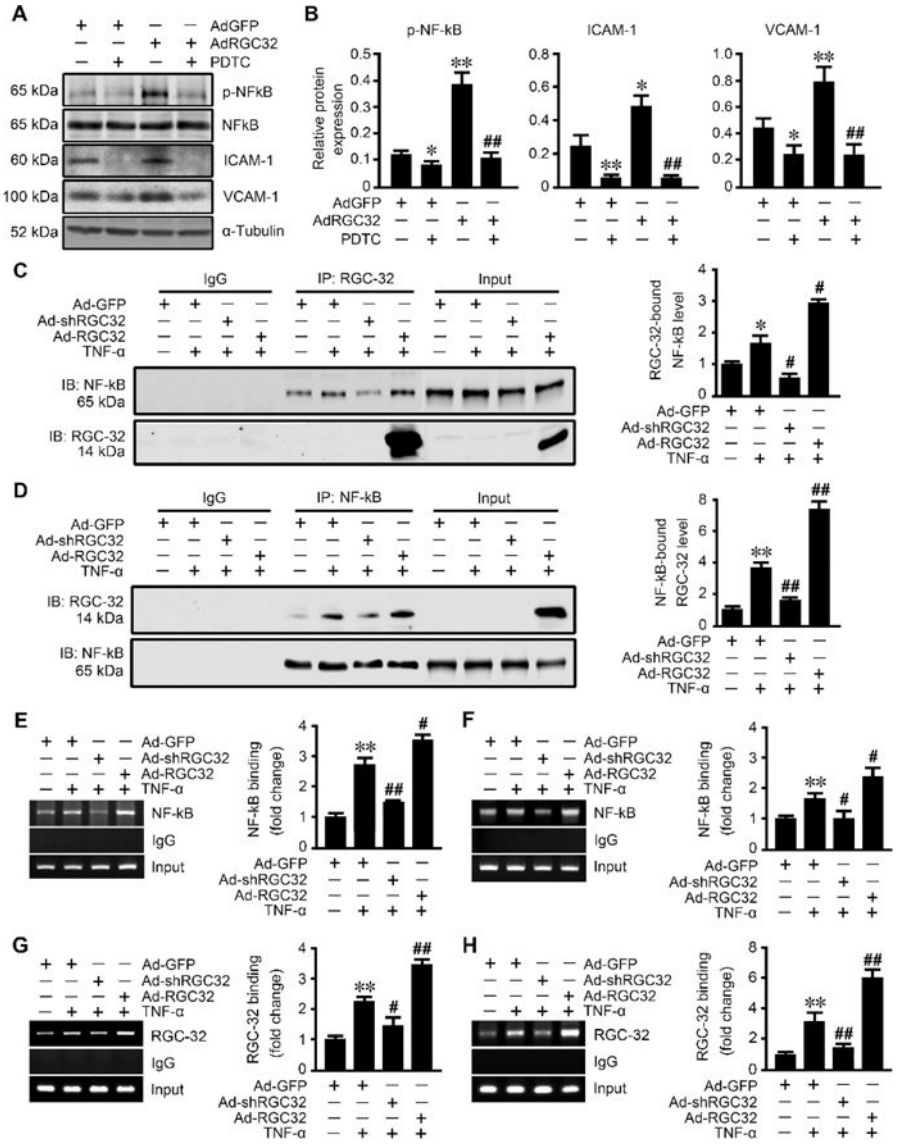


**Figure 6. RGC-32 mediated endothelial ICAM-1 and VCAM-1 expression through NF-κB signaling**

**A-B**, HUVECs were pretreated with vehicle or 25 μM PDTC and transduced with Ad-GFP or Ad-RGC32 for 48 hours. ICAM-1 and VCAM-1 protein expression was detected by Western blot and normalized to α-tubulin level. Phosphorylation of NF-κB p65 was normalized to the total NF-κB p65 level. *$P$<0.05, **$P$<0.01 compared with Ad-GFP groups, $^{\#\#}P$<0.01 compared with Ad-RGC32 alone groups. **C-H**, HUVECs were transduced with Ad-GFP, Ad-shRGC32, or Ad-RGC32 for 48 hours, and then treated with vehicle or 20 ng/ml TNF-α for 6 hours. **C-D**, CoIP was performed with IgG, RGC-32, or NF-κB p65 antibody as indicated. The immunoprecipitates were immunoblotted (IB) with NF-κB p65 and RGC-32 antibody. **E-H**, ChIP assay was performed to detect the NF-κB and RGC-32 binding enrichment to ICAM-1 (**E** and **G**) or VCAM-1 (**F** and **H**) promoter, as measured by RT-PCR and qPCR. *$P$<0.05, **$P$<0.01 compared with Ad-GFP groups, $^{\#}P$<0.05, $^{\#\#}P$<0.01

compared with Ad-GFP groups treated with TNF-α. All results are representative of at least three independent experiments.